Global Analysis of Herpes Simplex Virus Type 1 Transcription Using an Oligonucleotide-Based DNA Microarray†

S. W. STINGLEY,[1] J. J. GARCIA RAMIREZ,[2] S. A. AGUILAR,[1] K. SIMMEN,[3]
R. M. SANDRI-GOLDIN,[1] P. GHAZAL,[2]* AND E. K. WAGNER[1]*

*Department of Molecular Biology and Biochemistry, University of California, Irvine,[1] Departments of
Immunology and Molecular Biology, The Scripps Research Institute, La Jolla,[2] and
The R. W. Johnson Pharmaceutical Research Institute, San Diego,[3] California*

Received 21 June 2000/Accepted 10 August 2000

More than 100 transcripts of various abundances and kinetic classes are expressed during phases of productive and latent infections by herpes simplex virus (HSV) type 1. To carry out rapid global analysis of variations in such patterns as a function of perturbation of viral regulatory genes and cell differentiation, we have made DNA microchips containing sets of 75-mer oligonucleotides specific for individual viral transcripts. About half of these are unique for single transcripts, while others function for overlapping ones. We have also included probes for 57 human genes known to be involved in some aspect of stress response. The chips efficiently detect all viral transcripts, and analysis of those abundant under various conditions of infection demonstrates excellent correlation with known kinetics of mRNA accumulation. Further, quantitative sensitivity is high. We have further applied global analysis of transcription to an investigation of mRNA populations in cells infected with a mutant virus in which the essential immediate-early $\alpha27$ (U_L54) gene has been functionally deleted. Transcripts expressed at 6 h following infection with this mutant can be classified into three groups: those whose abundance is augmented (mainly immediate-early transcripts) or unaltered, those whose abundance is somewhat reduced, and those where there is a significant reduction in transcript levels. These do not conform to any particular kinetic class. Interestingly, levels of many cellular transcripts surveyed are increased. The high proportion of such transcripts suggests that the $\alpha27$ gene plays a major role in the early decline in cellular gene expression so characteristic of HSV infection.

The application of robotic microarraying techniques and laser-based image analysis has led to the development of DNA microarrays as a powerful tool for the global analysis of transcriptional responses of cells and microorganisms to perturbations in their environment such as stress (23, 47). The major source of DNA sequences for gene probes are currently cloned fragments, often amplified by PCR, but the relatively affordable synthesis of oligonucleotides long enough to afford appropriate hybrid stability and specificity (especially strand specificity) provides another approach. The use of defined oligonucleotide probes is especially attractive for the synthesis of microarrays specific for large viral pathogens, and Chambers et al. have reported a highly effective chip for global assay of human cytomegalovirus (human herpesvirus 5) using 75-mers (6). Indeed, this is the first description of a chip for a human pathogen. We have used this approach to synthesize a first-generation chip for the analysis of herpes simplex virus type 1 (HSV-1; human herpesvirus 1) of equivalent specificity and sensitivity.

Despite HSV replication and pathogenesis being phenomenologically well characterized (see references 53 to 56 for recent reviews emphasizing our point of view), there are plenty of gaps remaining in our understanding of its mechanistic basis. A rapidly resolving initial acute infection is followed by lifelong latent infection interspersed with sporadic reactivation episodes. HSV (as well as other herpesviruses) has a promoter-rich genome. During infection, specific promoters mapping at cognate genes mediate transcript expression. All data suggest that the coordinate regulation of expression of viral transcripts must involve the transcriptional machinery of the cell in toto. A major factor in the control of viral gene expression is the differential activity of promoters whose functional architecture is, in large part, responsible for controlling access to the transcriptional machinery of the cell. A second major factor in the regulation of expression of at least some viral genes is the alteration of posttranscriptional processing and transport of viral transcripts mediated by the activity of the immediate-early $\alpha27$ (ICP27) gene (42, 50). In this light and in the most general sense, regulation of HSV gene expression can be understood only in light of normal cellular transcription processes. While viral regulatory proteins operate to drastically alter the regulatory environment of the host cell during infection, their effects are manifest through existing cellular transcription factors and enzymes. Two well-studied examples of this fact are the initial activation of immediate-early viral regulatory genes by the potent *trans* activator α-TIF (U_L48) in conjunction with the action of a cellular adapter, Oct-1 (2, 58). And, the global transcriptional activator $\alpha4$ (ICP4), itself related to a cellular transcriptional activator (26), functions through stabilization of the binding of TFIID (10).

Global analysis of viral transcription under various conditions of infection will provide a powerful tool for further analysis of the HSV transcription program. We have applied sequence-based computer programs and our own databases to select sets of 75-nucleotide (nt) oligonucleotide sequences within

* Corresponding author. Mailing address for P. Ghazal: Departments of Mol. Biol. & Immunology, The Scripps Research Institute, 10055 N. Torrey Pines Rd., La Jolla, CA 92037. Phone: (858) 784-8678. Fax: (858) 784-9272. E-mail: ghazal@scripps.edu. Mailing address for E. K. Wagner: Department of Molecular Biology & Biochemistry, University of California, Irvine, 19172 Jamboree Rd., Irvine, CA 92697. Phone: (949) 824-5370. Fax: (949) 824-8551. E-mail: ewagner@uci.edu.

the HSV-1 genome (Genbank accession number NC001806) that are specific for the expression of individual viral transcripts. With an eye toward efficient synthesis of oligo(dT)-primed cDNA from RNA isolated from infected cells and tissues, we have probed the 52 polyadenylation sites known to function in the viral genome. More than half of the total viral transcripts are terminated with a unique polyadenylation site and thus can be uniquely specified with unique oligonucleotides adjacent to the polyadenylation sites. Accordingly, we arrayed these oligonucleotide probes on glass slides to generate a first-generation HSV-1 DNA microarray (HSV-chip). We have included a set of cellular oligonucleotide probes specific for a number of transcripts expressed from genes involved in cellular response pathways to provide an indicator of the response of the cell to virus infection under the conditions surveyed here.

We have used nick-translated viral DNA and cloned DNA fragments to optimize hybridization conditions and demonstrate the high specificity of this first-generation chip. We next generated oligo(dT)-primed cDNA labeled with Cy3- and Cy5-tagged fluorescent nucleoside derivatives generated from RNA isolated from cells infected and mock infected with HSV under various conditions, which influence the class of viral and cellular genes expressed. Thus, inhibition of de novo protein synthesis allows only expression of immediate-early genes, blockage of DNA replication inhibits expression of strict late genes, isolation of RNA at short times after infection results in high enrichment of early-phase transcripts, and isolation of RNA at a time of high rates of viral genome replication results in preferential recovery of late transcripts. The data presented here demonstrate that all classes of viral transcripts can be detected with good efficiency and very high specificity. Further, a limited set of cellular transcripts are induced following infection against a general background of virus-mediated shutoff of cellular gene expression. Measurement of the transcript population abundant in cells infected with a mutant of HSV-1 lacking a functional α27 (U_L54) gene revealed significantly different patterns of both viral and cellular genes.

MATERIALS AND METHODS

Selection and synthesis of oligonucleotide probes for the microarray. We followed published methodology (6, 47) to select a total of 99 individual 75-mers specific for individual HSV-1 transcription units. The positions of these oligonucleotides vis-à-vis the sequence of the genome of HSV-1 strain 17syn^+ are shown in Table 1. Our overall criteria for choice were as follows. We concentrated within 300 nt of the polyadenylation [poly(A)] signal for each transcript group because synthesis of cDNA using oligo(dT) primers with the bulky Cy3- and Cy5-tagged dCTP produces a product of average length of less than 500 nt. We then used the commercial Oligo6 program (Molecular Biology Insights, Cascade, Colo.) to scan these sequences and chose 75-mers whose base composition was near the average for the region as a whole and which did not display a large deal of self-homology that would lead to the formation of hairpin loops. Oligonucleotides thus chosen had G+C contents ranging from 50 to 80%. Two nonoverlapping oligomers were chosen for all abundant transcripts. Cell genes (GenBank notation) and accession numbers from which specific oligonucleotides were synthesized are as follows: ATF3, L19871; JUNC, J04111; CCNA cyclinA, M963390; JUND, NM005354; MAPK, NM002745; MBP-2, X65644; MHC-1, NM005514; MHC-2, AH002891; CvDC25A, NM001789; mlkBa, L32976; CvDC25B, NM004358; NFAT1, U43341, CYCLIN B, M25753; NF-Y, NM002505; CYCLIND1, NM001758; NF-YB, NM006166; E2F1, AH006643; N-SHC, D84361; E2F2, NM004091; p107, NM002895; p130 HSP130K, X76061; p15, U19796; E2F5, NM001951; p16, U12820; EGR1, NM001964; p18, J04991; ELK, NM005229; p19, U71364; FAS-1A, D38122; p21 (PAK1), NM002576; FAS-2, M67454; p27, NM005532; FOS, NM005252; p300, NM001429; FRA1, NM005438; p38 (RPP38), NM006414; p53, AAF63442; p65NFkB, A42017; RARa1, NM000964; RARb, NM000965; RXRb, AF120161; IL6, S56892; INFα/β, M54886; SRF, NM003131; FAS-1A, D38122; STAT2, NM005419; IRF1, NM002198; STAT5, NM003252; ISG 54K E1, M14659; STAT6, NM003153; ISG 54K E2, M14660; TAP1, L21207; ISG F3g p48, NM000107; JAK3, NM000215; JNK, NM002750; JUN B, NM002229; UNG, NM003362; and JUN-Bta, U20734.

Oligonucleotides were synthesized by using a PE Perseptive Bio-System (Fra-

mingham, Mass.) Expedite MOSS DNA synthesizer with membrane columns. Synthesized gene target oligonucleotides were cleaved, deprotected, and purified by standard procedures. Probe oligonucleotides were transferred in triplicate to 96-well master plates at a concentration of 1 μg/μl in 3× SSC (1× SSC is 0.15 M NaCl plus 0.015 M sodium citrate) for robotic deposition.
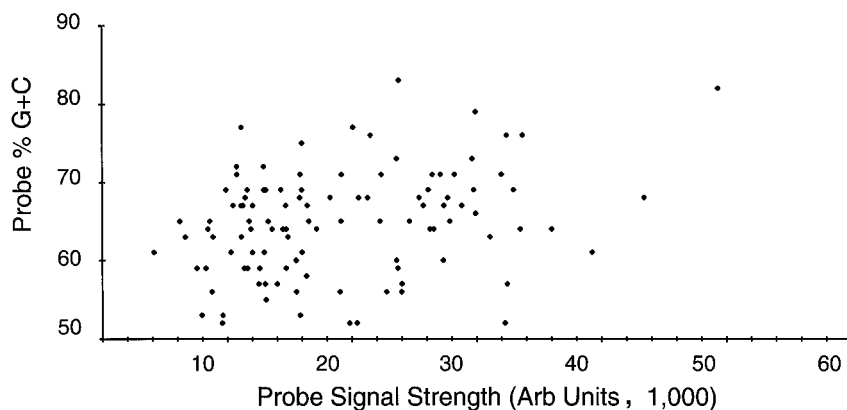
FIG. 1. Demonstration of microarray specificity. The maximum hybridization signal in arbitrary (Arb) units attained with nick-translated HSV-1 DNA fluorescently labeled with Cy3dCTP and hybridized with the probes listed in Table 1 at 68°C is plotted against the G+C content of each probe.

Generation of microarrays, hybridization, and scanning. The deposition printing of DNA was carried out as described in reference 6. The microarrayer tip delivered approximately 4 nl per spot on prescreened custom-made polylysine-coated glass slides (46, 47; see also http://www.gene-chips.com/). Microarrays were hybridized for 16 h in 5× SSC–0.2% sodium dodecyl sulfate (SDS) at 68°C under coverslips with combined Cy5dCTP and Cy3dCTP (Amersham)-labeled DNA. The entire assembly was enclosed in a custom-made hybridization chamber. After hybridization, the microarray slide assembly was washed for 5 min in 1× SSC–0.2% SDS at room temperature for 5 min, 5 min in 0.1× SSC–0.2% SDS at room temperature, and 1 min in 0.1× SSC, spun dry in a low-speed centrifuge, and scanned. Microarrays were scanned by using a confocal laser ScanArray 4000 (General Scanning, Inc.) system. Data were collected at a maximum resolution of 10 μm/pixel with 16 bits of depth by using Quantarray software (General Scanning).

Cells and virus. We used HSV-1 (17syn⁺) for kinetic and control experiments. The 27lacZ mutant, in which a β-galactosidase cassette was inserted into the α27 (U_L54) gene to inactivate the protein, was constructed from the KOS strain, and control experiments with this virus were done with the wild-type (wt) parent (40, 49, 52). Cultures of 5×10^6 HeLa cells in 100-mm² plates were used for infections at a multiplicity of infection of 5 PFU/cell except where indicated otherwise. Cells were maintained at 37°C under 5% carbon dioxide in Eagle minimum essential medium containing 5% calf serum, 100 U of penicillin per ml, and 100 μg of streptomycin per ml.

RNA preparation, cDNA synthesis, and nick translation. We followed published procedures (11, 12, 24, 27, 31, 47, 56) to extract total RNA from infected and mock-infected cells. Virus was adsorbed for 30 min prior to addition of fresh overlay medium. For preparation of RNA from cycloheximide and phosphonoacetic acid (PAA)-treated cells, cells were pretreated with drug for 30 min prior to addition of virus, and drug was present in the virus inocula and overlay medium. At appropriate times, cultures were rinsed twice with ice-cold saline containing cycloheximide (50 μg/ml), scraped and deposited by low-speed centrifugation, and then extracted with guanidinium isothiocyanate. Extracted RNA was recovered by pelleting through a 5.7 M CsCl cushion by centrifugation for 16 h at 36,000 rpm in a Beckman SW41 rotor. RNA recoveries were approximately 200 μg per dish.

Fluorescence-labeled cDNA was prepared from 40-μg aliquots of total infected or mock-infected cell RNA by oligo(dT)-primed polymerization by using SuperScript II reverse transcriptase (Gibco-BRL). The pool of nucleotides in the labeling reaction consisted of 0.5 mM dGTP, dATP, and dTTP and 0.3 mM dCTP and fluorescent nucleotides (Cy3dCTP and Cy5dCTP; Amersham) at 0.1 mM. All experiments with virus-infected cell RNA or nick-translated viral DNA were carried out with the Cy3 label. Nick-translated DNA was synthesized in a mixture of 50 mM Tris-HCl (pH 7.2), 10 mM MgSO₄, and 0.1 mM dithiothreitol with 20 μm dATP, dTTP, dGTP, and Cy3dCTP. Fluorescence-labeled DNA was purified by chromatography through Microcon YM-30 columns (Amicon), then heat denatured for 2 min at 100°C, and incubated 20 to 30 min at 37°C before use. Hybridization was for 16 h at 68°C using 3× SSC–0.3% SDS under a glass coverslip. The array area was ca. 3 cm², and total hybridization volume was 20 μl.

RESULTS

Demonstration of hybridization specificity. We first established probe specificity. We hybridized chips with probes arrayed in triplicate with fluorescence-labeled nick-translated HSV DNA at 65, 68, and 72°C. We found no appreciable cross-hybridization to the cellular probes (data not shown). We

surveyed signal strength and plotted this versus G+C content of the probe. We found 68°C to be the best overall temperature, since it provided the strongest hybridization signals with no obvious correlation with G+C content (Fig. 1). Specificity was further checked by hybridization with nick-translated DNA from a plasmid in which only the high-G+C joint and repeat regions were cloned (an XhoI/EcoRI fragment spanning 0.81 to 0.86 map units); here only the joint and repeat regions represented in the clone provided a hybridization signal (data not shown).

Patterns of RNA expression as a function of conditions of infection. We isolated RNA from HeLa cells infected with HSV-1 (5 PFU/cell) under various conditions of infection. Results of hybridization of cDNA generated from RNA isolated from cells 3 h postinfection (p.i.) in the presence of cycloheximide (50 μg/ml), 2 h p.i. with no drug, 4 h p.i. in the presence of PAA (300 μg/ml) to inhibit viral DNA replication, and 8 h p.i. with no drug are shown in Table 2. Each value is the median of values from two completely separate experiments with a total number of probes spotted per transcript unit ranging from 6 to 12. No normalization between experiments was carried out, but each group of signals was compared to mock-infected controls, and the difference was ranked. The statistical analysis is described in the table footnotes, and a significant value (i.e., one showing a significant difference) was one with a rank of ≤0.05.

Clearly, different individual transcripts reach their maximum levels under different conditions of infection. These levels generally reflect the kinetics of expression of the transcripts as determined by numerous individual Northern blot, RNase protection, and primer extension analyses carried out by us as well as many other laboratories over the past two decades (29, 37, 45, 53, 55, 62). The statistical significances of the differences between early (2-h) and late (8-h) hybridization patterns are also listed in Table 2.

The average (mean) values from individual cycloheximide, 2-h, and 8-h RNA experiments are shown in Fig. 2. In the absence of appreciable protein synthesis (the result of incubation of HeLa cells with 50 μg of cycloheximide per ml), only the immediate-early genes α0 (ICP0), α4, U_L54 (α27), U_S1 (α22 [ICP22]), and U_S12 (α47 [ICP47]) are expressed at high levels. Low levels of the DNA polymerase transcript (U_L30) and large and small subunits of ribonucleotide reductase (U_L39/40) are discernible in this experiment; of this yield, only the U_L39/40 signal is significantly different from the mock-infected control ($P = 0.0002$). Expression of both low-abun-

TABLE 2. Transcript abundance in HeLa cells infected with HSV-1 under various conditions

Transcript, kinetic class[b]	Remarks (reference[s])[c]	Abundance[a]								Rank[d]
		Cycloheximide RNA		PAA RNA		2-h RNA		8-h RNA		2-h vs 8-h
		Signal	Rank	Signal	Rank	Signal	Rank	Signal	Rank	
ICP34.5, L	Neurovirulence (7, 8)	289	0.0081	1,412	0.0158	3,138	0.0002	2,075	0.0002	0.2174
ICP0, IE	*trans* activator	5,838	0.0000[e]	4,321	0.0002	8,398	0.0000	8,521	0.0000	0.9556
RHA6, L	1,400 nt 3′ of LAT cap (13)	189	0.0077	1,721	0.0002	775	0.0002	2,017	0.0002	0.0002
ORF-X, L	Low abundance (48)	149	0.0011	1,351	0.1610	736	0.0011	2,945	0.0002	0.0002
ORF-Y, L	Low abundance (48)	152	0.0160	2,021	0.0300	1,171	0.0002	4,347	0.0002	0.0011
U_L1/2, L/E	gL/uracil DNA glycosylase (48)	335	0.2817	5,002	0.0003	9,284	0.0000	6,786	0.0000	0.1943
U_L3, L	Unknown	381	0.6535	2,109	0.1197	2,393	0.0002	1,488	0.0586	0.0173
U_L1X, ?	Antisense to U_L1, low abundance (48)	418	0.2691	1,896	0.0001	2,688	0.0000	5,028	0.0001	0.0000
U_L4/5, L/E	Unknown/part of helicase-primase complex	408	0.1681	1,821	0.0000	4,192	0.0000	8,868	0.0000	0.0024
U_L6/7, L/?	Capsid maturation/unknown	293	0.0030	2,512	0.0000	2,420	0.0000	10,248	0.0000	0.0000
U_L8/9, E/E	Part of helicase-primase complex/origin binding	198	0.0648	2,371	0.0000	3,623	0.0000	7,181	0.0000	0.0000
U_L10, L	gM	203	0.0171	2,017	0.0098	2,512	0.0001	7,956	0.0004	0.0000
U_L11/14, L/E/L/L	U_L12 (alkaline exonuclease)/U_L13 (protein kinase)	385	0.7781	1,656	0.0000	5,209	0.0003	3,796	0.0000	0.0000
U_L15, L	Spliced-DNA packaging	307	0.1029	923	0.0027	2,332	0.0000	5,108	0.0000	0.0006
U_L16/17, L/L	Unknown/cleavage and packaging of DNA	235	0.0023	1,043	0.5028	1,827	0.0000	7,272	0.0000	0.0000
U_L18/20, L/L/L	VP23 (triplex)/VP5 major capsid protein/membrane associated	173	0.0114	2,497	0.0003	5,373	0.0000	11,972	0.0000	0.0000
U_L19/20, L/L	Very weak poly(A) site (9)	266	0.0002	839	0.0059	2,671	0.0000	2,171	0.0038	0.0349
U_L21, L	Auxiliary virion maturation function (?)	227	0.0345	1,812	0.0001	3,703	0.0000	5,032	0.0000	0.0119
U_L22, L	gH	377	0.6975	2,806	0.0010	9,455	0.0003	5,178	0.0000	0.2581
U_L23, E	Thymidine kinase	288	0.1182	1,602	0.4043	6,230	0.0033	3,799	0.0002	0.0000
U_L24, L	Unknown regulated poly(A) site (18)	141	0.0440	1,321	0.0048	4,300	0.0034	5,182	0.0056	0.3674
U_L25/26/26.5, L/L	Capsid maturation/maturational protease/scaffolding protein	248	0.0005	2,306	0.0002	4,989	0.0001	7,453	0.0000	0.0173
U_L27/28, E/L	gB/capsid maturation	278	0.0012	2,286	0.0000	4,270	0.0001	3,607	0.0000	0.6544
U_L29, E	Single-stranded DNA binding protein	277	0.0012	2,065	0.0000	3,180	0.0000	2,804	0.0651	0.9111
U_L30, E	DNA polymerase	1,029	0.0273	3,823	0.0002	4,308	0.0000	1,523	0.0117	0.0001
U_L31/34, L/L/L/L	Nuclear phosphoprotein/capsid maturation/capsid maturation/phosphoprotein	662	0.1221	1,970	0.0000	1,961	0.0062	4,569	0.0005	0.0000
U_L35, L	Capsomer tips	392	0.0577	3,162	0.0000	3,249	0.0001	4,075	0.0019	0.1074
U_L36, (E)/L	ICP1/2 very large tegument protein (two transcripts, smaller encodes partial ORF)	282	0.0002	1,332	0.0024	1,023	0.0072	6,666	0.0005	0.0000
U_L37, E	Tegument phosphoprotein	338	0.0102	2,259	0.0001	1,050	0.0003	4,959	0.0000	0.0000
U_L38, L	Efficiency of poly(A) site usage varies with cell type (1, 15)	374	0.0014	1,881	0.0000	518	0.1206	5,818	0.0007	0.0000
U_L39/40, E/E	Large and small subunits of ribonucleotide reductase	2,387	0.0002	8,781	0.0001	13,665	0.0000	8,890	0.0000	0.0357
U_L41, L	Virion-associated host shutoff protein	341	0.0024	2,022	0.0000	1,111	0.0036	3,217	0.0002	0.0000
U_L42/U_L43.5, E/L	Part of helicase-primase complex/tegument (57)	256	0.0011	2,990	0.0015	3,699	0.0002	10,491	0.0001	0.0003
U_L43, E(?)	Unknown (5)	175	0.0029	1,955	0.0001	470	0.0037	1,453	0.7666	0.0000
U_L44/45, L/L	gC/virion associated	422	0.0022	3,647	0.0000	2,033	0.0001	10,352	0.0003	0.0000
U_L46/47, L/L	Modulates α-TIF (61)	1,137	0.2912	3,088	0.0000	4,126	0.0000	6,503	0.0000	0.1227
U_L48, L	α-TIF	238	0.0477	4,160	0.0000	4,731	0.0000	10,413	0.0000	0.0001
U_L49/.49.5, E/L	Tegument protein/unknown	399	0.0787	4,014	0.0006	4,837	0.0003	7,524	0.0000	0.1535
U_L50, E	dUTPase	294	0.0011	4,757	0.0000	2,557	0.0010	6,782	0.0000	0.0008
U_L51, L	Unknown	149	0.0118	1,661	0.0001	976	0.0096	11,146	0.0000	0.0000
U_L52/53, E/L	Helicase-primase complex/gK	255	0.0036	881	0.0040	722	0.1008	1,504	0.0000	0.0000
U_L54, IE	RNA transport/inhibition of splicing	12,696	0.0000	9,458	0.0000	11,889	0.0000	6,915	0.0000	0.0000
U_L55, E?	Unknown, pathogenesis (3, 38)	102	0.0000	2,184	0.0016	1,000	0.0358	2,225	0.0005	0.0000
U_L56, E?	Unknown, pathogenesis (3, 38)	212	0.7744	1,237	0.0052	904	0.0430	1,752	0.0040	0.0736
LAT/(OrfO/P) poly(A) site	Reactivation/modulate ICP0, ICP22/modulate ICP4?) (4, 32, 33, 59)	604	0.1786	1,031	0.0157	475	0.0532	1,499	0.0093	0.0002
ICP4, IE	Broad-range *trans* activator	6,562	0.0241	3,789	0.0000	4,688	0.0008	7,626	0.0000	0.0172
U_S1, IE	Host range	21,001	0.0000	17,356	0.0000	18,250	0.0000	12,606	0.0000	0.1714
U_S2, E?	Unknown	380	0.7366	1,222	0.0094	2,036	0.2530	3,750	0.0001	0.0003
U_S3/4, E/E?	Protein kinase/gG	364	0.0773	4,625	0.0003	8,562	0.0000	6,639	0.0000	0.0207
U_S5/6/7, E/E	gJ/gD (entry)/gI (Fc binding)	443	0.1131	7,129	0.0001	12,655	0.0000	8,598	0.0000	0.0344
U_S8/9, E/E	gE (Fc binding)/unknown	486	0.1692	11,934	0.0000	17,082	0.0000	9,113	0.0000	0.0000
U_S10/11/12, E/E/IE	Unknown/RNA binding phosphoprotein/α47 (inhibits MHC-I presentation) (60)	13,764	0.0000	7,692	0.0001	14,381	0.0000	10,203	0.0000	0.0636

[a] Signal intensities were determined by calculating the median of background-subtracted values for two independent experiments based on 6 or 12 replicates. P values reported with corresponding median values (Rank) were determined by ranking the replicate values for each sequence ($n = 6$ or 12) from both mock-infected and HSV-infected cells. The null hypothesis ($P = 1$), that mock and HSV groups are identical, was tested for the ranked values instead of the background-adjusted values by using Student's t test with two-tail distribution and assuming unequal variance. This procedure of applying Student's t test to the rank of the signals instead the signal values is an approximation to the nonparametric Mann-Whitney rank test (16).

[b] Early mapping and kinetic data are compiled in reference 45. L, late; IE, immediate early; E, early.

[c] General information concerning genetic functions can be found in reference 37.

[d] The null hypothesis is that the 2- and 8-h signals are the same.

[e] $P < 0.0001$.
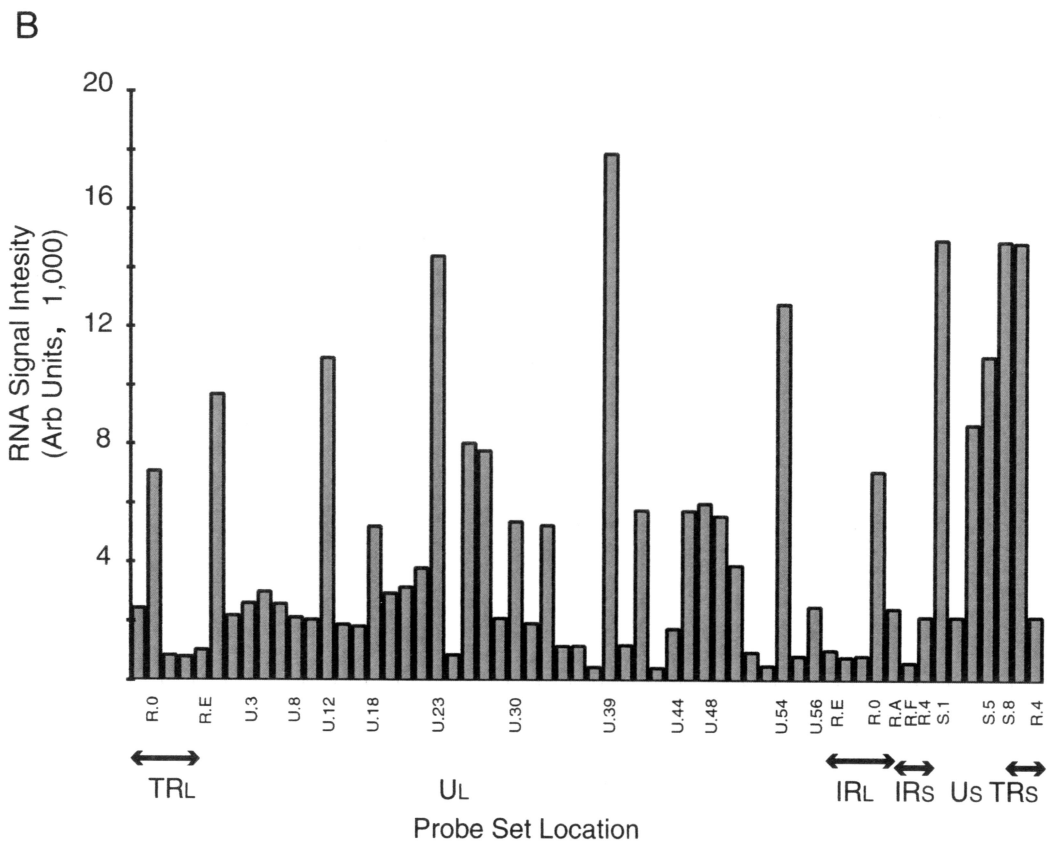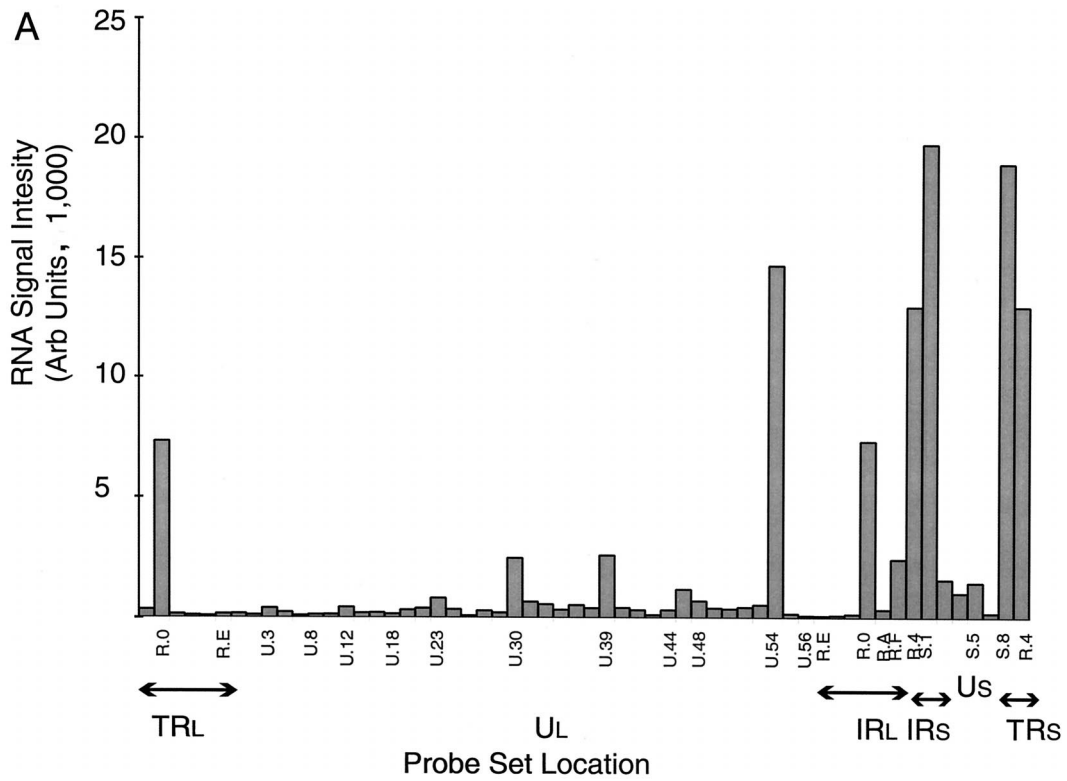
FIG. 2. Hybridization of oligo(dT)-primed cDNA synthesized from HeLa cells under various conditions of infection to an HSV-1 specific microarray. Each panel is based on a single experiment; a summary showing median values is shown in Table 2. (A) Hybridization of cDNA synthesized to RNA abundant in HeLa cells 3 h following infection in the presence of cycloheximide (50 μg/ml). (B) Hybridization of cDNA synthesized to RNA abundant in HeLa cells 2 h following infection. (C) Hybridization of cDNA synthesized to RNA abundant in HeLa cells 8 h following infection. Arb, arbitrary.
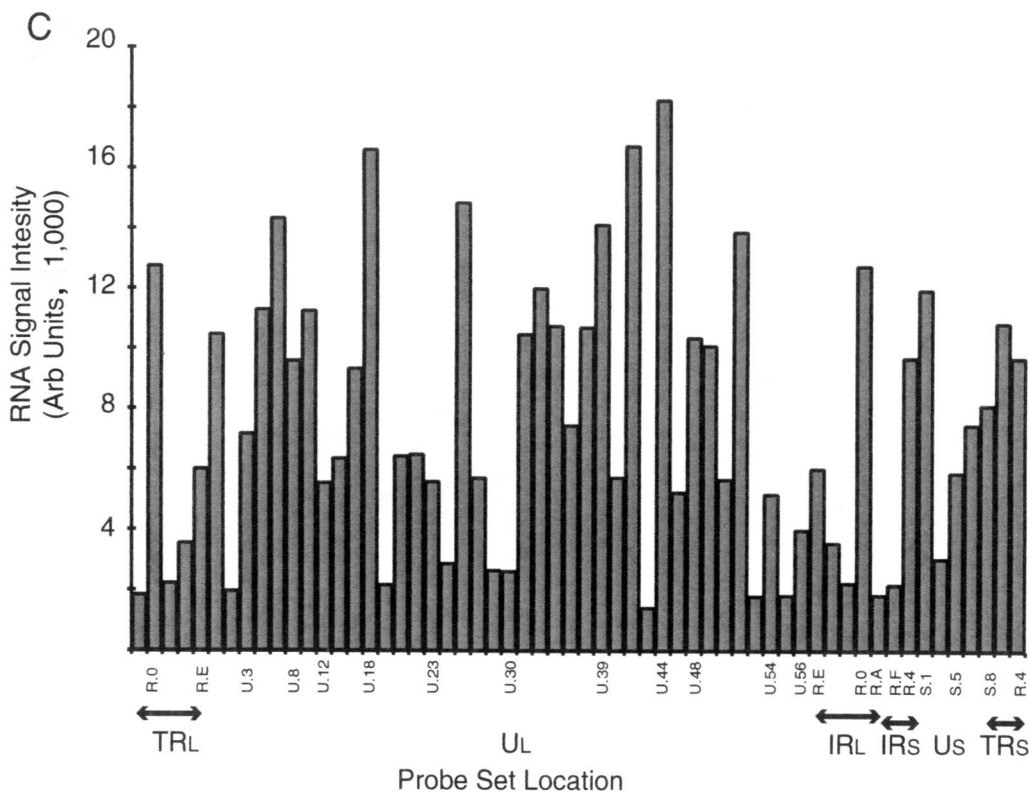
FIG. 2—Continued.

dance transcripts was eliminated by increasing the stringency of inhibition of protein synthesis through raising the inhibitor concentration to 100 μg/ml (data not shown). Under these conditions, expression of the α27 (U_L54) transcript is also markedly reduced. We also isolated RNA from rabbit skin cells infected at the same multiplicity and incubated for 3 h in the presence of the lower amount of inhibitor. There was no evident expression of transcripts detected by either the U_L30- or U_L39/40-specific probe, but the relative expression of the α27 transcript was comparable to that seen in HeLa cells at the same inhibitor concentration (data not shown).

The hybridization pattern due to the presence of RNA expressed at 2 h p.i. was, as expected, considerably more complex (Fig. 2B). The relative abundance of thymidine kinase (U_L23), the early alkaline exonuclease transcript (U_L12), DNA polymerase (U_L30), α27, and many of the early transcripts of the short unique region are evident. On the other hand, results for 8-h RNA hybridization (Fig. 2C) reveal the relative increase in abundance of both strict late and leaky late transcripts, including those hybridizing to the U.18 probe (containing the major capsids [U_L19]-encoding transcript), the strict late U_L38 capsid protein, and the gC- and U_L45-encoding transcripts revealed with the U.44 probe. In addition, the relative decline in abundance of some early transcripts such as thymidine kinase, α27, and DNA polymerase are notable.

While this analysis is generally consistent with the kinetic classification of individual transcripts arrived at both by analysis of stable transcripts and by incorporation of radioactive precursors as a measure of synthesis at a specific time or in the presence of metabolic inhibitors, there are some notable differences. One factor is a difference in the stability of viral transcripts in HeLa cells compared to rabbit skin cells, where

thorough transcription studies have been carried out. For example, we have extensively studied the properties of the promoter controlling the expression of the U_L37 transcript in HSV-infected rabbit skin cells (30, 62). All data demonstrate that this is a low-abundance early transcript controlled by a relatively weak promoter. Despite this, the level of this transcript increases in HeLa cells between 2 and 8 h (Table 2).

Continuous labeling using [^{32}P]orthophosphate experiments demonstrated that the 3.6-kb U_L37 transcript continues to accumulate in HeLa cells (1), and we confirmed that this difference is cell based by carrying out a comparative analysis of the ratio of cDNA generated from RNA isolated at late (7 h p.i.) and early (3 h p.i.) times in rabbit skin cells. Here, the abundance of this transcript declines as would be expected for an early transcript (Table 3). Both the similarities and differences between the ratios of RNA abundance at late versus early times following infection of HeLa and rabbit skin cells is readily apparent when the log_{10} of each ratio is plotted as shown in Fig. 3. The possible significance of other differences is considered in Discussion.

Global analysis of viral transcripts accumulating in the absence of the α27 gene product. The above results demonstrate the efficiency of the HSV-1 DNA microarray for detecting differential accumulation of viral transcripts as a function of conditions of infection. We also compared the relative abundance of viral transcripts in cells 6 h after infection with the *27lacZ* mutant of the KOS strain of HSV-1 versus the parental *wt* virus. The data in Table 4 show that there are generally three groups of transcripts. The first group evidenced expression near or above *wt* levels. Thus, in the mutant infections a total of 10 of the 52 transcript sets had a rank statistically equivalent to the *wt* level (i.e., $P \gg 0.05$), and one (ICP4) was

TABLE 3. Effect of the host cell on the ratio of HSV-1 transcripts at early and late times following infection

8-h/2-h signal, HeLa cells	Probe set	7-h/3-h signal, rabbit skin cells	8-h/2-h signal, HeLa cells	Probe set	7-h/3-h signal, rabbit skin cells
0.75	R.A	0.67	2.28	U.35	0.60
1.80	R.O	1.00	9.21	U.36	1.09
2.64	R.C	0.78	6.34	U.37	1.13
4.47	R.D	1.39	23.10	U.38	2.46
5.80	R.E	1.51	0.79	U.39	0.55
1.08	U.1	0.80	4.77	U.41	1.30
0.90	U.1X	0.15	2.90	U.42	1.54
2.74	U.3	3.93	3.25	U.43	2.85
3.78	U.4	1.16	10.38	U.44	1.80
5.56	U.6	1.09	0.91	U.46	0.91
4.51	U.8	0.52	1.73	U.48	0.64
5.46	U.10	1.88	1.81	U.49	0.73
0.51	U.12	0.66	1.45	U.50	0.85
3.35	U.15	1.14	14.40	U.51	2.02
5.10	U.16	2.06	3.51	U.52	1.04
3.19	U.18	1.91	0.41	U.54	0.46
0.74	U.19X	1.79	2.19	U.55	0.53
2.04	U.21	2.20	1.59	U.56	0.61
1.71	U.22	1.54	3.52	R.F	2.14
0.39	U.23	1.47	4.48	R.4	0.59
3.27	U.24	2.80	0.80	S.1	0.73
1.85	U.25	3.08	1.41	S.2	1.52
0.73	U.27	1.64	0.68	S.3	0.87
1.26	U.29	0.94	0.68	S.5	1.48
0.49	U.30	0.44	0.54	S.8	1.96
5.41	U.31	3.16	0.73	S.12	1.51

present at greater than the *wt* level ($P < 0.0001$). The majority (39 of 52) of transcript sets analyzed showed a statistically significant reduction in abundance following infection with the mutant virus. Of these, about half (21 of 39) were reduced by a factor of 5 or more. As detailed in Discussion, the effects seen are generally consistent with a number of other studies using different approaches.

Response of selected cellular transcripts to HSV-1 infection. As outlined in Materials and Methods, we designed the present DNA microarray to contain selected human genes, a number of which are expressed by transcripts known to be responsive to perturbations of the cellular environment. Not unexpectedly, we found that the maximum signal for most cellular genes probed was significantly less than seen for the viral transcripts, but the 57 genes listed in Table 5 all provided a signal during at least one of the conditions tested that was reproducibly above the background level seen with a control human cytomegalovirus probe (U_L124R) included as a negative control.

We first analyzed cellular mRNA abundance in HeLa cells immediately following the 30-min virus adsorption period with that compared to a mock-infected sample as a control for differential efficiency of detecting the infected cell Cy3 label versus the uninfected cell Cy5 label. This 0-h time point control was used to establish a baseline for the expected normal level of cellular transcript. We then analyzed cellular mRNA abundance in HeLa cells at 2 and 8 h after infection with the 17*syn*$^+$ strain of HSV-1. The average data from two independent experiments are shown in Table 5, and the $\log_{10}$ of each ratio of

TABLE 4. Abundance of HSV transcripts at 6 h p.i. in cells infected with the *27lacZ* mutant[a]

Probe set	*27lacZ* Signal	*27lacZ* Rank (P)	KOS Signal	KOS Rank	Mutant vs KOS rank[b]	Probe set	*27lacZ* Signal	*27lacZ* Rank	KOS Signal	KOS Rank	Mutant vs KOS rank
R.A	784	0.0576	2,420	0.0062	0.0000[c]	U.35	1,099	0.0001	5,026	0.0000	0.0000
R.O	**6,855**	**0.0000**	**6,588**	**0.0000**	**0.8285**	U.36	557	0.9017	3,232	0.0000	0.0001
R.C	473	0.8994	1,296	0.3714	0.0576	U.37	777	0.0187	3,184	0.0000	0.0000
R.D	458	0.9664	1,792	0.2447	0.0568	**U.38**	**4,343**	**0.0000**	**6,559**	**0.0000**	**0.1080**
R.E	**1,014**	**0.0545**	**1,787**	**0.0000**	**0.1264**	**U.39**	**7,952**	**0.0000**	**9,303**	**0.0000**	**0.5991**
U.1	4,423	0.0000	7,911	0.0000	0.0340	U.41	706	0.2629	3,255	0.0000	0.0007
U.1X	600	0.6425	1,765	0.0072	0.0452	U.42	710	0.0027	5,913	0.0000	0.0000
U.3	735	0.2103	4,675	0.0000	0.0000	U.43	723	0.2887	1,974	0.0000	0.0002
U.4	971	0.0014	6,005	0.0000	0.0000	U.44	1,512	0.0011	5,744	0.0000	0.0000
U.6	632	0.4950	6,767	0.0000	0.0000	U.46	964	0.0000	4,642	0.0000	0.0000
U.8	601	0.1233	4,505	0.0000	0.0000	U.48	909	0.0004	8,040	0.0000	0.0000
U.10	1,450	0.0000	4,749	0.0000	0.0000	U.49	991	0.0011	5,831	0.0000	0.0000
U.12	627	0.6874	1,336	0.0632	0.0000	U.50	1,407	0.0000	7,546	0.0000	0.0000
U.15	726	0.2105	2,716	0.0000	0.0004	U.51	560	0.8286	3,750	0.0000	0.0000
U.16	389	0.2914	2,054	0.0000	0.0000	U.52	628	0.8284	1,731	0.0000	0.0000
U.18	367	0.1240	4,042	0.0000	0.0000	**U.54**	**676**	**0.2346**	**3,561**	**0.0000**	**0.0000**
U.19X	435	0.4021	9,223	0.0000	0.0000	U.55	574	0.4009	2,437	0.0000	0.0000
U.21	353	0.2004	1,801	0.0000	0.0000	U.56	505	0.3837	1,455	0.0039	0.0000
U.22	421	0.5772	2,767	0.0000	0.0001	**R.F**[d]	**663**	**1.0000**	**843**	**0.4187**	**0.3183**
U.23	1,984	0.0156	6,349	0.0000	0.0000	R.4	8,205	0.0000	2,930	0.0000	0.0000
U.24	1,043	0.0218	3,919	0.0000	0.0014	**S.1**	**17,194**	**0.0000**	**15,490**	**0.0000**	**0.8045**
U.25	373	0.2769	3,586	0.0000	0.0000	S.2	650	0.7100	4,664	0.0000	0.0000
U.27	2,098	0.0345	6,367	0.0000	0.0030	S.3	1,166	0.0103	5,010	0.0000	0.0000
U.29	**3,030**	**0.0000**	**3,729**	**0.0000**	**0.9753**	S.5	2,287	0.0000	9,329	0.0000	0.0002
U.30	**1,812**	**0.0000**	**1,051**	**0.0395**	**0.6198**	S.8	3,623	0.0000	9,464	0.0000	0.0761
U.31	2,211	0.0000	3,616	0.0000	0.0010	**S.12**	**6,451**	**0.0000**	**8,189**	**0.0000**	**0.7568**

[a] Signal intensities were determined by calculating the median of background-subtracted values for three independent experiments based on 9 or 18 replicates. P values reported with corresponding median values (Rank) were determined by ranking the replicate values for each sequence ($n = 9$ or 18) from both mock- and HSV-infected cells. The null hypothesis, that mock and HSV groups are identical, was tested for the ranked values instead of the background adjusted values by using Student's t test with two-tail distribution and assuming unequal variance. This procedure of applying Student's t test to the rank of the signals instead the signal values is an approximation to the nonparametric Mann-Whitney rank test (16). Boldface entries are comparable or increased in *27lacZ* (an insertion mutant expressing a chimeric transcript [40, 49, 52]) infection compared to *wt* KOS infection.

[b] The null hypothesis is that the mutant (*27lacZ*) and *wt* signals are the same.

[c] Signal too low under conditions used for a meaningful conclusion.
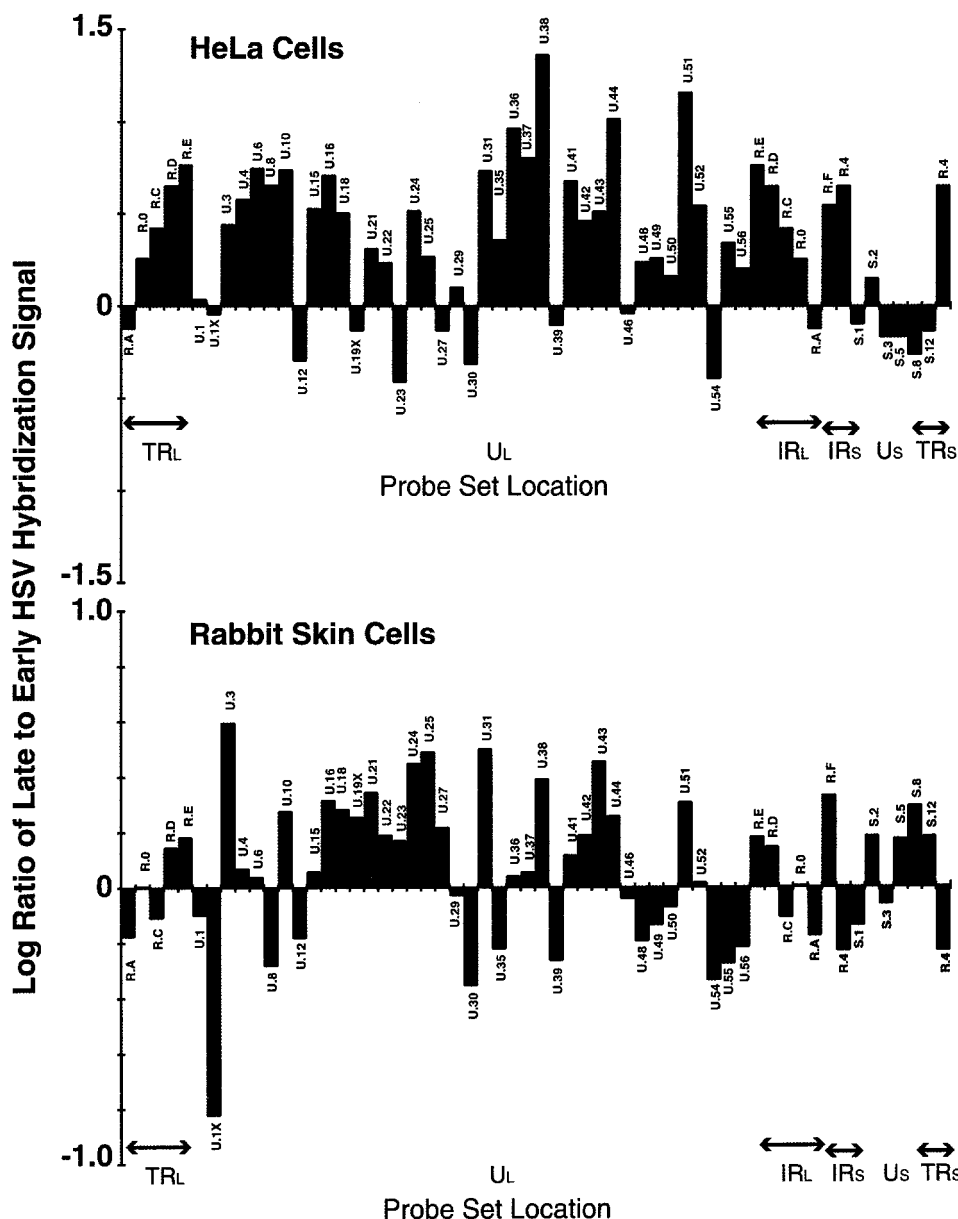
[d] $P < 0.0001$.

FIG. 3. The $\log_{10}$ of the ratio of late to early infected HeLa and rabbit skin cell viral RNA is plotted to emphasize time-specific differences in abundance. The late and early times for HeLa cells are 8 and 2 h p.i., respectively; those for rabbit skin cells are 7 and 3 h p.i.

infected cell to uninfected cell abundance is shown graphically in Fig. 4A. Notably, against (an expected) general decline in cellular mRNA abundance, transcripts representing database entries ATF3, INFα/β, ISG 54K E2, JUNC, N-SHC, and TAP1 were present at levels near or above control values at either the 2- or 8-h time point.

The effect of infection of the *27lacZ* mutant on cellular transcript abundance was more varied (Table 5 and Fig. 4B). The major decline in transcript abundance is not seen at 6 h following infection with this mutant, but some transcripts are markedly reduced compared to control values. These include CYCLIND1, IL6, JUNC, MHC-2, p107, p130 HSP130K, and RARb. Transcripts specific for INFα/β, JUNBta, JUND, N-SHC, p15, p16, p27, and TAP1 were significantly increased in abundance compared to control values.

DISCUSSION

The data presented here demonstrate the power of the approach of using defined oligonucleotide probes for the HSV-1 DNA microarray. Such a microarray provides an additional convenient addition to the available tools for the investigation of HSV transcription. Our immediate goal was to construct a microarray with the minimum number of probes necessary to uniquely detect all groups of HSV transcripts as well as diagnostic host cell genes perturbed by viral infection. Our criteria for choosing appropriate probes included position relative to the transcript polyadenylation site, lack of internal repeat or reiterated sequences, and base composition near the average for the region of DNA being transcribed. The first-generation chip that we have constructed demonstrates that these criteria are sufficient for the choice of probes displaying excellent spec-

ificity and adequate sensitivity for assaying the expression of a large number of viral genes under various conditions of infection. Despite its value, however, it is important to note that further probes and cDNA synthesis regimens will be necessary to fully optimize the specificity of detection of individual viral genes transcribed. Our ultimate goal is to apply this microarray technology to direct analysis of viral gene expression in specific tissues and in animals.

Since the general patterns of HSV-1 gene expression during productive infection are well known, as is the transcription program and relationship of transcripts to genomic sequence, we used viral RNA isolated under varied conditions of infection to serve as our basic platform for assaying the capabilities of the present microarray for detailed global analysis of viral transcript abundance.

Microarray analysis of HSV mRNA abundance. General patterns of viral gene expression and gene function have been derived from studies where relatively large quantities of cultured cells are infected under selected and/or optimized conditions (see references 53 and 55 for recent reviews emphasizing our own point of view on this broadly studied topic). The summary microarray data presented in Table 2 are in good general agreement with the far more laboriously formulated kinetic classification of viral transcripts based on Northern blot, hybrid selection, RNase protection, primer extension, and metabolic labeling studies carried out over the past two decades. There are, of course, some areas of nonagreement. Some of these are due to lack of resolution of the current chip, since coterminal transcripts of different kinetic classes cannot be distinguished. Also, and not surprisingly, some discrepancies are seen with transcripts expressed with low abundance. And it is clear that the actual cell in which the studies are carried out has a significant bearing on the relative proportion of viral transcripts recovered at any given time or under any particular conditions of infection. Thus, HeLa cells require quite high levels of cycloheximide (100 μg/ml) to suppress low-level expression of one or two nominally early HSV transcripts. Also, the early $U_L 37$ transcript continues to accumulate late in infected HeLa cells but not rabbit skin cells (Table 3). Another example can be seen in the level of the prototypical immediate-early α4 transcript, which does not change much between 2 and 8 h in HeLa cells but decreases markedly in rabbit skin cells (compare Tables 2 and 3). While most differences in accumulation can be ascribed to differential mRNA stability in the various cells infected with the virus, other differences may reflect differences in the efficiency of shutoff of early transcription at late times in various cell types. Indeed, the sharp shutoff with rabbit skin cells is the major reason that we have used them for our continuing kinetic studies (62).
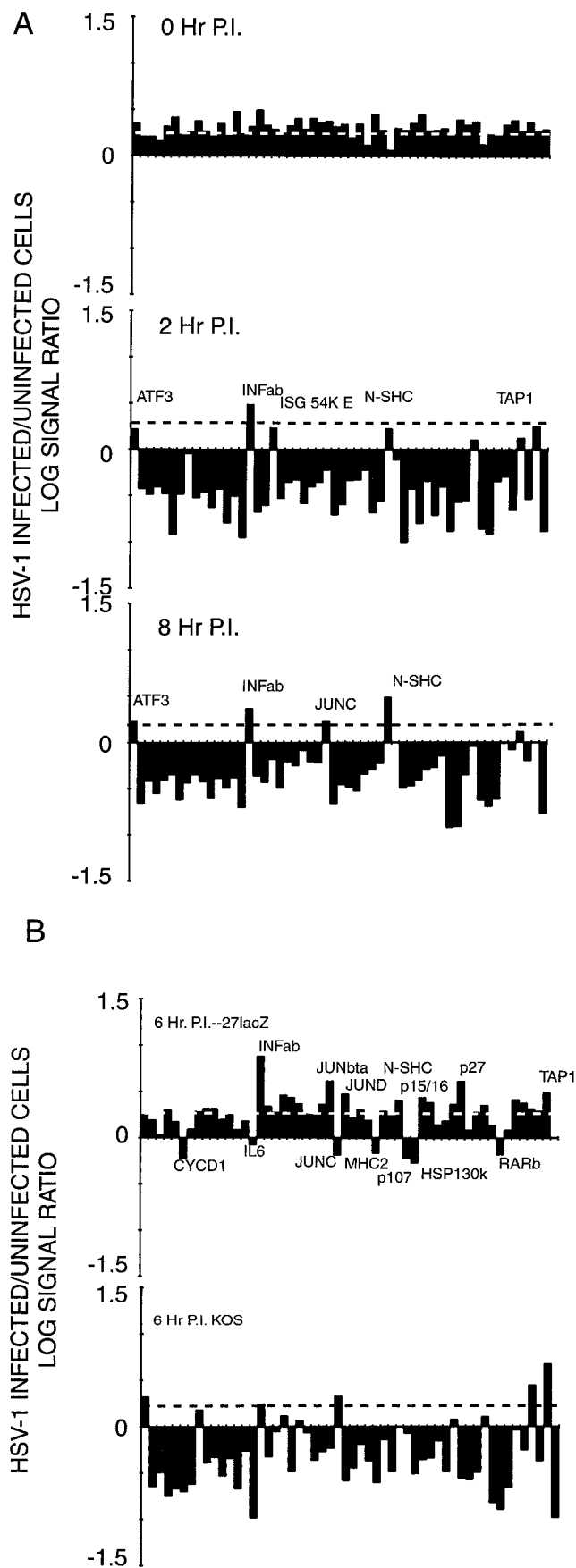
Most of these relatively few discrepancies will be readily resolved by increasing the resolution of the microarray using random oligomers as well as oligo(dT) to prime cDNA synthesis and by carefully characterizing the nature of viral transcription and RNA accumulation as a function of the cell infected. Some discrepancies, however, are the result of inadequacies in our current kinetic classification schemes. The classification of three basic groups of transcripts (and the proteins encoded by them) is based on one or another measures of transcript abundance in infections where virus-induced protein and DNA synthesis are blocked with metabolic inhibitors. The subclassification into leaky late and strict late, early and delayed early, etc., is based on relative abundance at specific times before and after genome replication. Such a scheme fails to take into account the real situation where some transcripts are expressed at low levels throughout infection and neither amplified nor

TABLE 5. Relative abundance of transcripts under various conditions of HSV-1 infection of HeLa cells

Cell transcript	Ratio, infected cell/uninfected cell transcript abundance[a]				
	0 h p.i.	2 h p.i.	6 h p.i., KOS	8 h p.i.	6 h p.i., 27lacZ
ATF3	2.23	1.66	2.09	1.71	1.80
CCNA cyclinA	1.60	0.37	0.23	0.22	1.55
CvDC25A	1.61	0.32	0.32	0.38	1.07
CvDC25B	1.44	0.39	0.18	0.28	1.98
CYCLIN B	2.07	0.33	0.21	0.39	1.47
CYCLIND1	2.62	0.11	0.13	0.19	0.97
E2F1	1.70	0.33	0.24	0.24	1.23
E2F2	1.80	0.90	1.50	0.37	1.90
E2F5	2.38	0.30	0.41	0.45	2.05
ELK	1.85	0.34	0.46	0.38	2.05
FAS-1A	1.63	0.24	0.29	0.25	1.56
FAS-2	2.23	0.37	0.45	0.41	1.77
FOS	1.64	0.16	0.21	0.32	1.21
FRA1	3.01	0.31	0.55	0.41	1.51
IL6	1.72	0.11	0.10	0.20	0.85
INF α/β	2.08	3.06	1.73	2.30	7.62
INT6	3.11	0.21	0.47	0.43	2.17
IRF1	2.14	0.25	0.88	0.37	1.87
ISG 54K E1	1.94	1.69	1.29	0.65	2.89
ISG 54K E2	1.76	0.30	0.33	0.32	2.71
ISG F3g p48	2.11	0.44	1.16	0.62	2.32
JAK3	2.55	0.46	0.85	0.56	1.78
JNK	1.95	0.26	0.43	0.82	1.77
JUN B	2.55	0.39	0.54	0.62	2.30
JUNBta	2.30	0.44	0.58	0.60	4.09
JUNC	2.36	0.60	2.13	1.71	0.65
JUND	2.08	0.20	0.26	0.22	2.96
MAPK	2.20	0.25	0.36	0.35	1.64
MBP-2	1.57	0.46	0.64	0.33	1.99
MHC-1	2.23	0.47	0.43	0.30	1.55
MHC-2	1.31	0.60	0.25	0.45	0.69
mlkBa	2.83	0.21	0.72	0.51	1.92
NFAT1	1.90	0.28	0.33	0.59	1.73
NF-Y	1.61	0.15	0.16	0.27	1.25
NF-YB	1.80	0.13	0.18	0.26	1.27
N-SHC	1.16	1.67	1.00	3.03	2.56
p107	1.98	0.87	1.07	0.88	1.49
p130 HSP130K	1.90	0.14	0.12	0.21	0.99
p15	2.28	0.37	0.44	0.34	2.72
p16	2.80	0.16	0.46	0.39	2.40
p18	1.88	0.45	0.70	0.51	1.38
p19	1.90	0.19	0.33	0.53	1.52
p21 (PAK1)	2.00	0.39	1.19	0.71	2.31
p27	1.70	0.13	0.28	0.12	4.11
p300	2.47	0.27	0.27	0.12	1.22
p38 (RPP38)	2.18	0.28	0.32	0.45	1.88
p53	2.22	0.18	0.26	0.27	1.41
p65NFkB	2.36	1.26	1.27	0.90	2.26
RARa1	1.33	0.14	0.15	0.24	1.36
RARb	1.72	0.12	0.13	0.20	0.66
RXRb	1.70	0.45	0.22	0.24	1.21
SRF	2.19	0.50	0.92	0.98	2.59
STAT2	2.43	0.22	0.56	0.83	2.40
STAT5	1.85	1.33	2.79	1.29	2.06
STAT6	2.35	0.29	0.43	0.63	1.96
TAP1	1.84	1.78	4.72	0.99	3.12
UNG	1.94	0.13	0.10	0.17	1.01

[a] Based on at least two separate experiments.

shut off. This would appear to be the case for LAT (latency-associated transcript) and its truncated 5′-colinear polyadenylated transcript detected by probe sets R.C and R.F, respectively. Further, the levels of others transcripts are modulated posttranscriptionally. Other variations are also evident. For example, expression of the ICP34.5 protein has been classified as strict late (essentially requiring viral genome replication for expression), yet our experiments demonstrate that the tran-

FIG. 4. Abundance of selected cellular transcripts under various conditions of HSV-1 infection of HeLa cells. The relative abundance of transcripts hybridizing to the cellular probes used in this study is shown in Table 5. The $\log_{10}$ of the ratio of the signal seen in mock-infected to infected cells is plotted here. (A) Relative levels of cellular transcripts present under various conditions of infection with the 17syn[+] strain of HSV-1. The dashed line is the average ratio of mock-infected to infected cell signal for RNA isolated immediately following a 30-min virus adsorption period (top). (B) Effect of the $\alpha27$ (U_L54) immediate-early protein on cellular RNA abundance. The dashed line shows the average values of the 0-h control in panel A. The top panel shows the ratio of abundance of cellular RNAs in HeLa cells 6 h following infection and mock infection with the 27lacZ mutant of the KOS strain of HSV-1; the bottom panel shows the same ratio for cells infected and mock infected with the wt parental KOS strain.

script encoding it detected by probe set R.A is present at essentially equivalent levels at 2 h and 8 h. While the expression of this transcript is somewhat reduced in the presence of the DNA replication inhibitor PAA, it clearly does not fit the criteria of a strict-late transcript such as seen with U_L38 and $U_L44/45$ detected by the U.38 and U.44 probe sets, respectively.

Our survey of the relative abundance of viral transcripts expressed during infection with the 27lacZ mutant virus, in which the posttranscriptional regulatory protein $\alpha27$ (U_L54) has been inactivated, provides an excellent example of some of the advantages as well as limitations of using global quantitative analysis to form a complete picture of the situation inside the infected cell. Work from a number of laboratories has consistently shown that this protein has a major role in posttranscriptional regulation of viral RNA both through inhibition of splicing and by mediating the transport of a subset of viral transcripts from the nucleus to the cytoplasm in infected cells. This observation is based on a comparison in various cell types of the relative levels of $\alpha4$, $\alpha0$, $\alpha47$ (U_S12), U_L8 (helicase-primase), U_L19 (major capsid protein), U_L23 (thymidine kinase), U_L24, U_L27 (gB), U_L29 (major DNA binding protein), U_L30 (DNA polymerase), U_L38 (capsid protein), U_L41 (virion-associated shutoff protein), U_L44 (gC), U_L52 (helicase-primase), U_S6 (gD), and U_S11 (RNA binding protein) on polyribosomes as well as the ratio of viral transcripts in the nucleus versus the cytoplasm (18–21, 34–36, 41, 52). While we will need to use polysome-associated and nuclear and cytoplasmic RNA fractions for a complete comparison, generally the results of these studies are consistent with those presented in Table 4. Thus, increases in the levels of $\alpha4$ and $\alpha47$ (U_S12) were evident (19–21). Despite this overall consistency, we did not see the marked reduction in levels of U_L30 (DNA polymerase) and U_L52 (helicase-primase) transcripts reported (52). Also, DNA microarray analysis demonstrated an increased signal using the U.38 probe set specific for the U_L38 transcript in contrast to the complete absence of full-length transcript on polyribosomes noted by Hibbard and Sandri-Goldin (21). In other work, however, these same workers found that 3′ probes specific for U_L38 mRNA detected a 0.4-kb transcript in 27lacZ-infected cells, while 5′ probes detected nothing (M. K. Hibbard and R. M. Sandri-Goldin, unpublished data). Such a result suggests the stable accumulation of a misprocessed form of this transcript in mutant-infected cells. Such stable RNA fragments may also account, in part, for the other discrepancies noted here.

While it is clear that greater probe resolution and RNA fractionation will be required to fully characterize the specific transcripts accumulating during infections with mutants lacking functional $\alpha27$ (U_L54) protein using DNA microarray technology, the resolution of the present chip is still sufficient to add new information. Thus, the accumulation of the $\alpha4$ and

α47 (U$_S$12) transcripts is reflected by a similar increase in the level of α22 (U$_S$1) mRNA (Table 5). This suggests that the α27 (U$_L$54) protein may play a role in modulating levels of these immediate-early transcripts during the normal course of infection. The increase in abundance of transcripts detected by the U.30 and U.39 probe sets suggests important roles for them at the earliest stages of infection, and their apparent refractoriness to inhibition of protein synthesis in HeLa cells may be a related phenomenon. The statistically significant decrease in the abundance of ICP34.5 as seen with the loss of material hybridizing to probe set R.A suggests that the α27 protein also modulates the expression of this neurovirulence factor.

HSV-1 infection augments the abundance of some cellular transcripts. Hobbs and DeLuca (22), using an HSV mutant expressing primarily ICP0 and a human DNA microarray, noted induction of cellular transcripts. A similar array specific for 327 cellular genes was recently used to assess the effect of *wt* HSV infection in human embryonic lung cells (25). In agreement with these surveys, our much less extensive survey of cellular genes shown in Table 5 and Fig. 3A reveals a marked general decrease in transcript abundance. Exceptions include a limited number of stress response and cellular transcriptional regulatory genes. None of the transcripts surveyed were included in our group of cellular probes, but it is notable that the transcription factor ATF4 transcript abundance was increased since we found this to also be the case for the ATF3-specific transcript. In our studies, the INFα/β probe showed the most striking increase in cellular transcript abundance, and we also found increases in ISG 54K E2, JUNC, N-SHC, STAT5, and TAP1 transcripts consistent with a major effect on a limited number of stress response and regulatory genes.

A role of the α27 (U$_L$54) protein in the shutoff of host cell protein synthesis has been inferred from studies of protein synthesis in mutant virus-infected cells (36, 39, 50). Our analysis adds significant dimension to that picture by showing that the protein is directly involved in a decline in host mRNA abundance. Despite the general lack of decline of host cell transcripts, no correlation with extensive splicing was noted, and several were clearly reduced during infection with the regulatory mutant. Reductions in the levels of MHC (major histocompatibility complex) class II may reflect a role of α47 (U$_S$12) protein, although its primary function appears to be in the MHC class I pathway (17). Decreases in CYCLIND1, IL6, JUNC, p107, p130, HSP130K, and RARb transcripts must reflect the specific function(s) of other viral genes.

When adjusted for the appropriate controls, the abundance of only a few cellular transcripts increased during infection with the mutant virus. While similar to those increased in *wt* infections, the set was not identical. These results suggest that the α27 (U$_L$54) protein plays a role in the induction or stabilization of specific cellular genes following infection. This role may be related to its differential effect on the abundance and stability of only a subset of viral transcripts. It will be of interest to determine whether such transcripts contain common structural motifs.

Conclusions. As useful as the application of DNA microarray analysis is and will continue to be in studying viral gene expression in cultured cells, such infection does not necessarily reflect the process of virus infection and spread in the host. The most promising application of HSV-specific chips will be in analysis of viral replication in reactivation from latent infection and infection of a specific organ or cell type. Further, techniques are now available for collection of individual neurons and laser dissection of individual cells or extremely small samples of differentiated tissue and for the amplification of RNA in such tissues (14, 28, 43, 44, 46, 51). The power of the

approach will be augmented by assaying an increasing collection of cellular genes (both human and those specific for the animal model being studied) chosen to represent those whose expression is modulated by the stress of viral infection. The broad patterns of HSV and critical cellular gene expression exhibited under various conditions of infection and under the influence of defined modification of critical regulatory genes will illuminate potential critical points in the course of virus replication in the whole animal. Those differentiated cells and tissues where there is a critical restriction of virus replication are precisely the points where it can be expected that the full panoply of viral regulatory circuits must operate to optimum effect. They will provide important experimental subjects for further regulatory studies.

REFERENCES

1. **Anderson, K. P., R. J. Frink, G. B. Devi-Rao, B. H. Gaylord, R. H. Costa, and E. K. Wagner.** 1981. Detailed characterization of the mRNA mapping in the *Hin*dIII fragment K region of the herpes simplex virus type 1 genome. J. Virol. **37:**1011–1027.
2. **Arnosti, D. N., C. M. Preston, M. Hagmann, W. Schaffner, R. G. Hope, G. Laughlan, and B. F. Luisi.** 1993. Specific transcriptional activation *in vitro* by the herpes simplex virus protein VP16. Nucleic Acids Res. **21:**5570–5576.
3. **Ben-Hur, T., M. Moyal, A. Rosen-Wolff, G. Darai, and Y. Becker.** 1989. Characterization of RNA transcripts from herpes simplex virus-1 DNA fragment BamHI-B. Virology **169:**1–8.
4. **Bruni, R., and B. Roizman.** 1996. Open reading frame P—a herpes simplex virus gene repressed during productive infection encodes a protein that binds a splicing factor and reduces synthesis of viral proteins made from spliced mRNA. Proc. Natl. Acad. Sci. USA **93:**10423–10427.
5. **Carter, K. L., P. L. Ward, and B. Roizman.** 1996. Characterization of the products of the U$_L$43 gene of herpes simplex virus 1: potential implications for regulation of gene expression by antisense transcription. J. Virol. **70:**7663–7668.
6. **Chambers, J., A. Angulo, D. Amarantunga, H. Guo, Y. Jian, J. S. Wan, A. Bittner, K. Frueh, M. R. Jackson, P. A. Peterson, M. G. Erlander, and P. Ghazal.** 1999. DNA microarrays of the complex human cytomegalovirus genome: profiling kinetic class with drug sensitivity of viral gene expression. J. Virol. **73:**5757–5766.
7. **Chou, J., E. R. Kern, R. J. Whitley, and B. Roizman.** 1990. Mapping of herpes simplex virus-1 neurovirulence to gamma$_1$34.5, a gene nonessential for growth in culture. Science **250:**1262–1266.
8. **Chou, J., and B. Roizman.** 1994. Herpes simplex virus 1 gamma$_1$34.5 gene function, which blocks the host response to infection, maps in the homologous domain of the genes expressed during growth arrest and DNA damage. Proc. Natl. Acad. Sci. USA **91:**5247–5251.
9. **Costa, R. H., G. Cohen, R. Eisenberg, D. Long, and E. K. Wagner.** 1984. Direct demonstration that the abundant 6-kilobase herpes simplex virus type 1 mRNA mapping between 0.23 and 0.27 map units encodes the major capsid protein VP5. J. Virol. **49:**287–292.
10. **DeLuca, N. A., and M. J. Carrozza.** 1996. Interaction of the viral activator protein ICP4 with TFIID and through TAF250. Mol. Cell. Biol. **16:**3085–3093.
11. **Devi-Rao, G. B., J. S. Aguilar, M. K. Rice, H. H. Garza, Jr., D. C. Bloom, J. M. Hill, and E. K. Wagner.** 1997. Herpes simplex virus genome replication and transcription during induced reactivation in the rabbit eye. J. Virol. **71:**7039–7047.
12. **Devi-Rao, G. B., D. C. Bloom, J. G. Stevens, and E. K. Wagner.** 1994. Herpes simplex virus type 1 DNA replication and gene expression during explant induced reactivation of latently infected murine sensory ganglia. J. Virol. **68:**1271–1282.
13. **Devi-Rao, G. B., S. A. Goodart, L. B. Hecht, R. Rochford, M. K. Rice, and E. K. Wagner.** 1991. The relationship between polyadenylated and nonpoly-

adenylated herpes simplex virus type 1 latency-associated transcripts. J. Virol. **65:**2179–2190.

14. **Emmert-Buck, M. R., R. F. Bonner, P. D. Smith, R. F. Chuaqui, Z. Zhuang, S. R. Goldstein, R. A. Weiss, and L. A. Liotta.** 1996. Laser capture microdissection. Science **274:**998–1001.

15. **Flanagan, W. M., A. G. Papavassiliou, M. Rice, L. B. Hecht, S. J. Silverstein, and E. K. Wagner.** 1991. Analysis of the herpes simplex virus type 1 promoter controlling the expression of U_L38, a true late gene involved in capsid assembly. J. Virol. **65:**769–786.

16. **Glanz, S. A.** 1997. Primer of biostatistics. McGraw-Hill, New York, N.Y.

17. **Gustafsson, C. M., O. Hammarsten, M. Falkenberg, and P. Elias.** 1994. Herpes simplex virus DNA replication: a spacer sequence directs the ATP-dependent formation of a nucleoprotein complex at *ori_S*. Proc. Natl. Acad. Sci. USA **91:**4629–4633.

18. **Hann, L. E., W. J. Cook, S. L. Uprichard, D. M. Knipe, and D. M. Coen.** 1998. The role of herpes simplex virus ICP27 in the regulation of *UL24* gene expression by differential polyadenylation. J. Virol. **72:**7709–7714.

19. **Hardwicke, M. A., and R. M. Sandri-Goldin.** 1994. The herpes simplex virus regulatory protein ICP27 contributes to the decrease in cellular mRNA levels during infection. J. Virol. **68:**4797–4810.

20. **Hardy, W. R., and R. M. Sandri-Goldin.** 1994. Herpes simplex virus inhibits host cell splicing, and regulatory protein ICP27 is required for this effect. J. Virol. **68:**7790–7799.

21. **Hibbard, M. K., and R. M. Sandri-Goldin.** 1995. Arginine-rich regions succeeding the nuclear localization region of the herpes simplex virus type 1 regulatory protein ICP27 are required for efficient nuclear localization and late gene expression. J. Virol. **69:**4656–4667.

22. **Hobbs, W. E., II, and N. A. DeLuca.** 1999. Perturbation of cell cycle progression and cellular gene expression as a function of herpes simplex virus ICP0. J. Virol. **73:**8245–8255.

23. **Iyer, V. R., M. B. Eisen, D. T. Ross, G. Schuler, T. Moore, J. C. F. Lee, J. M. Trent, L. M. Staudt, J. Hudson, Jr., M. S. Boguski, D. Lashkari, D. Shalon, D. Botstein, and P. O. Brown.** 1999. The transcriptional program in the response of human fibroblasts to serum. Science **283:**83–87.

24. **Jarman, R. G., E. K. Wagner, and D. C. Bloom.** 1999. LAT expression during an acute HSV infection in the mouse. Virology **262:**384–397.

25. **Khodarev, N. N., S. J. Advani, N. Gupta, B. Roizman, and R. R. Weichselbaum.** 1999. Accumulation of specific RNAs encoding transcriptional factors and stress response proteins against a background of severe depletion of cellular RNAs in cells infected with herpes simplex virus 1. Proc. Natl. Acad. Sci. USA **96:**12062–12067.

26. **Kretzschmar, M., K. Kaiser, F. Lottspeich, and M. Meisterernst.** 1994. A novel mediator of class II gene transcription with homology to viral immediate-early transcriptional regulators. Cell **78:**525–534.

27. **Lieu, P. T., and E. K. Wagner.** 2000. The kinetics of VP5 mRNA expression is not critical for viral replication in cultured cells. J. Virol. **74:**2770–2776.

28. **Luo, L., R. C. Salunga, H. Guo, A. Bittner, K. C. Joy, J. E. Galindo, H. Xiao, K. E. Rogers, J. S. Wan, M. R. Jackson, and M. G. Erlander.** 1999. Gene expression profiles of laser-captured adjacent neuronal subtypes. Nat. Med. **5:**117–122.

29. **McGeoch, D. J.** 1991. Correlation between HSV-1 DNA sequence and viral transcription maps, p. 29–48. *In* E. K. Wagner (ed.), Herpesvirus transcription and its regulation. CRC Press, Boca Raton, Fla.

30. **Pande, N. T., M. D. Petroski, and E. K. Wagner.** 1998. Functional modules important for activated expression of early genes of herpes simplex virus type 1 are clustered upstream of the TATA box. Virology **246:**145–157.

31. **Petroski, M. D., and E. K. Wagner.** 1998. Purification and characterization of a cellular protein that binds to the downstream activation sequence of the strict late U_L38 promoter of herpes simplex virus type 1. J. Virol. **72:**8181–8190.

32. **Randall, G., M. Lagunoff, and B. Roizman.** 1997. The product of ORF O located within the domain of herpes simplex virus 1 genome transcribed during latent infection binds to and inhibits *in vitro* binding of infected cell protein 4 to its cognate DNA site. Proc. Natl. Acad. Sci. USA **94:**10379–10384.

33. **Randall, G., and B. Roizman.** 1997. Transcription of the derepressed open reading frame P of herpes simplex virus 1 precludes the expression of the antisense γ_1 34.5 gene and may account for the attenuation of the mutant virus. J. Virol. **71:**7750–7757.

34. **Rice, S. A., and D. M. Knipe.** 1990. Genetic evidence for two distinct transactivation functions of the herpes simplex virus alpha protein ICP27. J. Virol. **64:**1704–1715.

35. **Rice, S. A., V. Lam, and D. M. Knipe.** 1993. The acidic amino-terminal region of herpes simplex virus type 1 alpha protein ICP27 is required for an essential lytic function. J. Virol. **67:**1778–1787.

36. **Rice, S. A., L. S. Su, and D. M. Knipe.** 1989. Herpes simplex virus alpha protein ICP27 possesses separable positive and negative regulatory activities. J. Virol. **63:**3399–3407.

37. **Roizman, B., and A. E. Sears.** 1996. Herpes simplex viruses and their replication, p. 2231–2295. *In* B. N. Fields, D. M. Knipe, R. M. Chanock, M. S.

38. **Rosen-Wolff, A., J. Scholz, and G. Darai.** 1989. Organotropism of latent herpes simplex virus type 1 is correlated to the presence of a 1.5 kb RNA transcript mapped within the BamHI DNA fragment B (0.738 to 0.809 map units). Virus Res. **12:**43–51.

39. **Sacks, W. R., C. C. Greene, D. P. Aschman, and P. A. Schaffer.** 1985. Herpes simplex virus type 1 ICP27 is an essential regulatory protein. J. Virol. **55:**796–805.

40. **Sandri-Goldin, R. M.** 1991. Analysis of the regulatory activities of the HSV-1 α protein ICP27, p. 77–104. *In* E. K. Wagner (ed.), Herpesvirus transcription and its regulation. CRC Press, Boca Raton, Fla.

41. **Sandri-Goldin, R. M.** 1998. ICP27 mediates HSV RNA export by shuttling through a leucine-rich nuclear export signal and binding viral intronless RNAs through an RGG motif. Genes Dev. **12:**868–879.

42. **Sandri-Goldin, R. M., M. K. Hibbard, and M. A. Hardwicke.** 1995. The C-terminal repressor region of herpes simplex virus type 1 ICP27 is required for the redistribution of small nuclear ribonucleoprotein particles and splicing factor SC35; however, these alterations are not sufficient to inhibit host cell splicing. J. Virol. **69:**6063–6076.

43. **Sawtell, N. M.** 1997. Comprehensive quantification of herpes simplex virus latency at the single-cell level. J. Virol. **71:**5423–5431.

44. **Sawtell, N. M., D. K. Poon, C. S. Tansky, and R. L. Thompson.** 1998. The latent herpes simplex virus type 1 genome copy number in individual neurons is virus strain specific and correlates with reactivation. J. Virol. **72:**5343–5350.

45. **Schaffer, P. A., E. K. Wagner, G. B. Devi-Rao, and V. G. Preston.** 1987. Herpes simplex virus, p. 93–98. *In* S. O'Brien (ed.), Genetic maps 1987. Cold Spring Harbor Laboratory, Cold Spring Harbor, N.Y.

46. **Schena, M., R. A. Heller, T. P. Theriault, K. Konrad, E. Lachenmeier, and R. W. Davis.** 1998. Microarrays: biotechnology's discovery platform for functional genomics. Trends Biotechnol. **16:**301–306.

47. **Schena, M., D. Shalon, R. W. Davis, and P. O. Brown.** 1995. Quantitative monitoring of gene expression patterns with a complementary DNA microarray. Science **270:**467–470.

48. **Singh, J., and E. K. Wagner.** 1993. Transcriptional analysis of the TR_L/U_L region of herpes simplex virus type 1. Virology **196:**220–231.

49. **Smith, I. L., M. A. Hardwicke, and R. M. Sandri-Goldin.** 1992. Evidence that the herpes simplex virus immediate early protein ICP27 acts post-transcriptionally during infection to regulate gene expression. Virology **186:**74–86.

50. **Soliman, T. M., R. M. Sandri-Goldin, and S. J. Silverstein.** 1997. Shuttling of the herpes simplex virus type 1 regulatory protein ICP27 between the nucleus and cytoplasm mediates the expression of late proteins. J. Virol. **71:**9188–9197.

51. **Thompson, R. L., and N. M. Sawtell.** 2000. Replication of herpes simplex virus type 1 within trigeminal ganglia is required for high frequency but not high viral genome copy number latency. J. Virol. **74:**965–974.

52. **Uprichard, S. L., and D. M. Knipe.** 1996. Herpes simplex ICP27 mutant viruses exhibit reduced expression of specific DNA replication genes. J. Virol. **70:**1969–1980.

53. **Wagner, E. K.** 1999. Herpes simplex virus—molecular biology, p. 686–697. *In* R. G. Webster and A. Granoff (ed.), Encyclopedia of virology. Academic Press, London, England.

54. **Wagner, E. K., and D. C. Bloom.** 1997. The experimental investigation of herpes simplex virus latency. Clin. Microbiol. Rev. **10:**419–443.

55. **Wagner, E. K., J. F. Guzowski, and J. Singh.** 1995. Transcription of the herpes simplex virus genome during productive and latent infection. Prog. Nucleic Acid Res. Mol. Biol. **51:**123–168.

56. **Wagner, E. K., M. D. Petroski, N. T. Pande, P. T. Lieu, and M. K. Rice.** 1998. Analysis of factors influencing the kinetics of herpes simplex virus transcript expression utilizing recombinant virus. Methods **16:**105–116.

57. **Ward, P. L., D. E. Barker, and B. Roizman.** 1996. A novel herpes simplex virus 1 gene, U_L43.5, maps antisense to the U_L43 gene and encodes a protein which colocalizes in nuclear structures with capsid proteins. J. Virol. **70:**2684–2690.

58. **Xiao, P., and J. P. Capone.** 1990. A cellular factor binds to the herpes simplex virus type 1 transactivator Vmw65 and is required for Vmw65-dependent protein-DNA complex assembly with Oct-1. Mol. Cell. Biol. **10:**4974–4977.

59. **Yeh, L., and P. A. Schaffer.** 1993. A novel class of transcripts expressed with late kinetics in the absence of ICP4 spans the junction between the long and short segments of the herpes simplex virus type 1 genome. J. Virol. **67:**7373–7382.

60. **York, I. A., C. Roop, D. W. Andrews, S. R. Riddell, F. L. Graham, and D. C. Johnson.** 1994. A cytosolic herpes simplex virus protein inhibits antigen presentation to CH8+ T lymphocytes. Cell **77:**525–535.

61. **Zhang, Y., D. A. Sirko, and J. L. C. McKnight.** 1991. Role of herpes simplex virus type 1 UL46 and UL47 in αTIF-mediated transcriptional induction: characterization of three viral deletion mutants. J. Virol. **65:**829–841.

62. **Zhang, Y. F., and E. K. Wagner.** 1987. The kinetics of expression of individual herpes simplex virus type 1 transcripts. Virus Genes **1:**49–60.

Hirsch, J. L. Melnick, T. P. Monath, and B. Roizman (ed.), Virology. Raven Press, New York, N.Y.